Agricultural Water Management
Manuscript Draft

Manuscript Number: AGWAT8375

Title: Eco-physiological response of citrus orchards to soil water deficit and application of FAO-56 model to identify crop water stress under Regulated Deficit Irrigation

Article Type: Research Paper

Keywords: FAO-56 model; Midday Stem Water Potential; Regulated Deficit Irrigation, Water stress function; Citrus

Abstract: Micro-irrigation is considered one of the most efficient water distribution systems and allows increasing water use efficiency if coupled with effective water-saving irrigation management strategies as regulated deficit (RDI) or partial root-zone drying (PRD) techniques. However, application of these strategies makes it crucial the real-time monitoring of soil and crop water status, in order to identify appropriate irrigation scheduling parameters (irrigation timing and doses) and to prevent irreversible damage of plant system and/or crop yield reductions.
Even if midday stem water potential (MSWP) is considered one of the most affordable indicator for direct determinations of crop water status, its measurement requires skilled operators, is destructive and time consuming, so that indirect estimations are desirable. In this direction, agro-hydrological models can be considered an easy-to-use tool for indirect evaluations of soil and crop water status.
At this aim the paper, after examining the eco-physiological response of citrus orchards to soil water deficit, assessed the potential of FAO-56 agro-hydrological model to identify the crop water stress under different irrigation management strategies.
Experiments carried out during three years (2009-2011) allowed identifying the crop water stress response to soil water deficit conditions, also confirming the schematization proposed in FAO-56 paper for citrus orchards. Moreover, after evaluating the similarity between the measured MSWP with the simulated crop water stress coefficient, Ks, it was proved the fairly good performance of FAO-56 agro-hydrological model to predict soil water content, from one side, and the crop response to different irrigation management strategies, from the other.
The obtained results evidenced that the crop water stress coefficient estimated by the model can be used as a suitable indicator to replace the tedious and time-consuming field measurements of MSWP.

Highlights

A strong correlation existing between the water stress integral and the applied irrigation depth.

Water stress integral can be used to predict the seasonal irrigation volumes to be provided when a desired crop stress level is required.

When the values of soil water depletion (*D*) are below a critical threshold of 20 mm, midday stem water potentials (*MSWP*) resulted linearly decreasing at increasing *D*, as a consequence of the gradually rising crop water stress.

FAO-56 model is able to predict, with reasonable accuracy, the average *SWC* in the root zone (RMSE=0.04 m^3 m^{-3})

Temporal variability of *MSWP* can be explained by the dynamic of simulated K_s.

Eco-physiological response of citrus orchards to soil water deficit and application of FAO-56 model to identify crop water stress under Regulated Deficit Irrigation

Giovanni Rallo[1*], Pablo González-Altozano[2], Juan Manzano-Juárez[3] and Giuseppe Provenzano[4]

1) PhD, Researcher, Dipartimento Scienze Agrarie, Alimentari e Agro-Ambientali, Università di Pisa, Via del Borghetto 80, 56124 Pisa, Italy. email: giovanni.rallo@unipi.it.
2) PhD, Professor, Departamento de Ingeniería Rural y Agroalimentaria, Universitat Politècnica de València, c/Camí de Vera s/n, 46022 València, Spain. email: pgaltozano@agf.upv.es
3) PhD, Professor, Departamento de Ingeniería Rural y Agroalimentaria, Universitat Politècnica de València, c/Camí de Vera s/n, 46022 València, Spain. email: juamanju@agf.upv.es
4) PhD, Professor, Dipartimento Scienze Agrarie e Forestali, Università degli Studi di Palermo, Viale delle Scienze 13, 90128 Palermo, Italy. email: giuseppe.provenzano@unipa.it

*Corresponding author, email: giovanni.rallo@unipi.it

Abstract

Micro-irrigation is considered one of the most efficient water distribution systems and allows increasing water use efficiency if coupled with effective water-saving irrigation management strategies as regulated deficit (RDI) or partial root-zone drying (PRD) techniques. However, application of these strategies makes it crucial the real-time monitoring of soil and crop water status, in order to identify appropriate irrigation scheduling parameters (irrigation timing and doses) and to prevent irreversible damage of plant system and/or crop yield reductions.

Even if midday stem water potential (*MSWP*) is considered one of the most affordable indicator for direct determinations of crop water status, its measurement requires skilled operators, is destructive

and time consuming, so that indirect estimations are desirable. In this direction, agro-hydrological models can be considered an easy-to-use tool for indirect evaluations of soil and crop water status.

At this aim the paper, after examining the eco-physiological response of citrus orchards to soil water deficit, assessed the potential of FAO-56 agro-hydrological model to identify the crop water stress under different irrigation management strategies.

Experiments carried out during three years (2009-2011) allowed identifying the crop water stress response to soil water deficit conditions, also confirming the schematization proposed in FAO-56 paper for citrus orchards. Moreover, after evaluating the similarity between the measured *MSWP* with the simulated crop water stress coefficient, K_s, it was proved the fairly good performance of FAO-56 agro-hydrological model to predict soil water content, from one side, and the crop response to different irrigation management strategies, from the other.

The obtained results evidenced that the crop water stress coefficient estimated by the model can be used as a suitable indicator to replace the tedious and time-consuming field measurements of *MSWP*.

Keywords

FAO-56 model, Midday Stem Water Potential, Regulated Deficit Irrigation, Water stress function, Citrus

1. Introduction

Water availability is one of the most limiting factors in worldwide agriculture, which represents the largest water-consuming sector.

Among typical Mediterranean crops, citrus represents the second largest fruit crops in the European Union. The main producing countries are Spain, Italy, Greece and Portugal, with a total surface slightly higher than 322,000 ha, corresponding to about 25% of the total acreage of fruit orchards (Eurostat, 2014). The most of these orchard productions are located in arid or semi-arid regions, where the growing season is usually dry. Due to the high crop water requirements and the large surface involved, there is an increasing interest to improve crop sustainability in order to optimize crop water use, to preserve the productivity maximizing the economic benefits, while maintaining environmental quality (Provenzano et al., 2013).

Moreover, ~~if~~ considering that the annual number of precipitation days and the annual precipitation are decreasing, as predicted by climate change scenarios for Mediterranean region (Smith et al., 2007), it is evident that implementation of strategies aimed to increase water use efficiency can no longer be postponed.

If micro-irrigation is considered the most efficient water distribution system and several researches have ~~been~~ proposed design procedure to improve field distribution uniformity (Barragan et al., 2006; Provenzano et al., 2007; Wu et al., 2006), a number of works have been emphasizing that "water-saving" management strategies, such as regulated deficit irrigation, RDI, (García-Tejero et al., 2010; Gasque et al., 2016; Rodrigues et al., 2008) and partial root-zone drying, PRD, (De la Hera et al., 2007; Marsal et al., 2008; Romero et al., 2012), can contribute to significant reductions of the seasonal crop needs and consequently to increase water use efficiency.

However, the most effective way to increase water use efficiency is the precise control of irrigation that should be supported by soil/plant-based water status indicators (leaf/stem water potential, sap flow, trunk diameter, infrared thermometry) aimed to identify appropriate irrigation scheduling

parameters (irrigation timing and doses). Under RDI, water is generally supplied at levels below full crop transpiration during specific periods of the growing season. Operating in this way it is possible to balance the plant vigor with the potential production (Costa et al. 2007; de Souza et al., 2005), by limiting the irrigation volumes. On the other hand, PRD method involves the exposure of half of the roots system in a drying state, while the remaining roots are wetted, so to alter the irrigated roots in time cycles. Application of these water saving strategies, however, makes it crucial to monitor crop water status in order to identify, in real time, the level of water stress to which the crop is subjected, so to avoid irreversible consequences to the crop, as well as the loss of productions.

Leaf water potential (*LWP*) is a commonly used variable to describe crop water status and, when measured at predawn or midday, represents an indicator of any instantaneous crop water stress condition. The cumulative integral of *LWP*, referred to a specific time or during certain phenological stages, represents a link between the short-term stress and the long-term growth response (Myers, 1988).

Even if the measurements of leaf water potential are considered one of the most affordable methods for direct determinations of crop water status, these determinations require skilled operators, are destructive and time consuming, so that indirect estimations are desirable. In this direction, agro-hydrological models can be considered as an easy-to-use tool for indirect evaluations of soil and crop water status, as recently demonstrated for olive groves by Rallo et al. (2014a), as well as to estimate other parameters related to the crop development (Minacapilli et al., 2009; Cammalleri et al., 2013).

However, the application of agro-hydrological models, require the preliminary calibration and validation of the algorithms used to schematize the different processes occurring in the Soil-Plant-Atmosphere continuum, based on site-specific experimental investigations.

For a long time, irrigation in citrus orchards has been scheduled according to the FAO method

described in the paper number 56 (FAO-56), by considering the single or dual crop coefficient approach (Allen et al., 1998). During the different phenological stages, crop coefficients can be chosen among tabular values or according to experimental results. However, this scheduling strategy has some uncertainty, particularly in citrus orchards where crop water use depends on tree light interception (Consoli et al., 2006) or crop load (Yonemoto et al., 2004).

González-Altozano and Castel (1999) proved that in citrus orchards, fruit drop is not very sensitive to soil water deficit applied during the phase-II of fruit growth and, if returning to the full water dosage for a sufficiently long period before harvesting, it is possible to compensate the fruit growth (Cohen and Goell, 1988). On the other hand, Hutton et al. (2007) evidenced that even if water restrictions are applied only during the linear phase of fruit development, severe plant water stress might reduce the final fruit size at harvest.

If from one side FAO-56 model has been diffusely applied, its potential to detect water stress conditions has not been largely investigated yet. For different crop systems in fact, model validation has been generally carried out based on the comparison between measured and estimated soil water contents (Sammis et al., 2012) without considering the actual crop water status.

Researches in this direction should allow to verify how water management can affect the different adaptive crop behavior to water stress under different irrigation water saving strategies and environmental conditions, avoiding wrong decisions in irrigation water management programs, mainly in those environments prone to drought.

The main objectives of the paper were: i) to investigate on the eco-physiological response of the citrus orchard to soil water deficit and ii) to assess the potential of FAO-56 agro-hydrological model to identify water stress conditions when the crop is maintained under Regulated Deficit Irrigation (RDI) applied only during the phase II of fruit growth.

After the initial model calibration, based on the comparison between measured and simulated soil water contents in the root zone, its ability to identify actual crop water stress in the periods of water

restriction was assessed according to the observed similarity between the temporal dynamic of the simulated water stress coefficient (K_s) with the measured midday stem water potentials, *MSWP*.

1.1. Description of FAO-56 model

FAO-56 model (Allen et al., 1998) simulates the root zone depletion, D_r, at a daily time step, according to a simple tipping bucket approach:

$$Dr_i = Dr_{i-1} - \left(P_i - RO_i\right) - I_i + ETa_i + DP_i \quad (1)$$

where D_{ri} (mm) and D_{ri-1}(mm) are the root zone depletions at the end of day *i* and *i-1*, P_i (mm) is the net precipitation, RO_i is the surface runoff, ET_{ai} (mm) is the actual evapotranspiration, I_i is the irrigation depth and DP_i (mm) is the deep percolation of water moving out of the root zone.

The domain of the depletion equation ranges between 0, occurring when the soil is at field capacity, to a maximum value related to the total plant available water, *TAW* (mm), evaluated as:

$$TAW = 1000\left(SWC_{fc} - SWC_{wp}\right)Z_r \quad (2)$$

where SWC_{fc} ($m^3\ m^{-3}$) and SWC_{wp} ($m^3\ m^{-3}$) are the soil water contents corresponding to field capacity and wilting point and Z_r (m) is the depth of the root system. The multiplicative coefficient adjusts the units in order to express *TAW* in mm.

When considering the dual crop coefficients approach, crop potential evapotranspiration, ET_c, evaluated in absence of soil water deficit, is obtained by multiplying the Penman-Monteith reference evapotranspiration, ET_0 (Allen et al. 1998) to a coefficient, $K_{cb} + K_e$, composed by two terms. The first, K_{cb}, is the basal crop coefficient accounting for the plant transpiration, whereas the second, K_e, is the soil evaporation (*E*) coefficient, accounting for the topsoil evaporation.

When soil water content in the root zone and in the evaporative layer drop below the relative critical levels, crop water stress and friction on soil evaporation phenomena occur and the amount of actual crop transpiration and soil evaporation are evaluated by multiplying K_{cb} and K_e, respectively, to a transpiration (K_s) and an evaporation (K_r) reduction coefficient. Analytically, actual

evapotranspiration can be evaluated as:

$$ETa = \left(K_s K_{cb} + K_r K_e\right) ET_{ref} \quad (3)$$

Both the coefficients K_s and K_r range between 0 and 1. In absence of crop water stress K_s=1, whereas under soil water limiting conditions, K_s<1. After a rainfall or following irrigation K_r is 1, and soil evaporation is maximum. As the soil evaporative layer dries, K_r becomes lower than one and evaporation decreases till reaching zero when no water is available for evaporation in the upper soil layer.

The reduction factor, K_s, is a function of the amount of water crop depleted from the root zone (D) and, when D exceeds the readily available water ($D>RAW$), can be calculated as:

$$K_s = \frac{TAW - Dr}{\left(1 - p\right)TAW} \quad (4)$$

The depletion coefficient, p, in eq. 4 accounts for the resistance of crop to water stress and the values corresponding to different crops are tabulated in the original publication (Allen et al. 1998). Considering that p depends on the atmospheric evaporative demand, a function for adjusting p for ET_c is usually applied (van Diepen et al., 1988).

In FAO-56 model, irrigation timing can be evaluated based on the management allowed depletion, *MAD* (Merriam, 1966), depending on management and economic factors in addition to the other eco-physiological factors influencing p. When irrigation is scheduled in absence of crop water stress, the value of *MAD* can be assumed equal to p. On the contrary, when irrigation is managed under water-deficit conditions, the *MAD* parameter is higher than p. This last circumstance is typical of the semiarid Mediterranean environments. The original algorithm proposed in the FAO-56 paper ("Appendix 8: Spreadsheet for applying the dual K_c procedure in irrigation scheduling") only permits to schedule full irrigation ($MAD=p$) and not considers crops maintained under water stress conditions. This circumstance represents a limitation in the Mediterranean environment, where water is often a limiting factor for crop production. For this reason, Rallo et al. (2012)

proposed a first amendment of the original algorithm to allow irrigation scheduling of arboreal crops maintained under soil water deficit conditions. The amendment allowed to separate the eco-physiological factor, affected by the crop stress, from the management allowed depletion term, that is related to the farmer choices and depends on unsystematic variables like the economic factors.

Moreover, for drought tolerant crops, it has been observed that a convex shape better represents the crop water stress function (Rallo and Provenzano, 2013), so that a further adjustment of FAO 56 model was proposed to improve its performance in the estimation of actual transpiration fluxes and soil water contents for drought tolerant crops under soil water deficit conditions (Rallo et al., 2014a).

2. Materials and Methods

2.1. Site description, experimental design and irrigation treatments

The field experiments were carried out during three years (from 2009 to 2011) in Senyera, Spain (39º 3' N, 0º 30' W, 23 m a.s.l), in a commercial citrus orchard planted with Navel orange (*Citrus sinensis* L. Osbeck) grafted onto Cleopatra mandarin trees (*Citrus reshni* Hort.). The orchard was planted in 1982 in a square configuration, with spacing between plants equal to 5 m.

Three treatments, including one full irrigation and two RDI and at least 8 plants per treatments excluding the borders, were applied in order to replace different amounts of irrigation needs, *IN*, obtained by multiplying reference evapotranspiration to the crop coefficient, K_c, after subtracting the precipitation of the period. Reference evapotranspiration was evaluated according to the Penman-Monteith equation, in the version modified by FAO (Allen et al., 1998), whereas the crop coefficient, K_c, was determined by using the site-specific polynomial equation, as a function of the measured canopy fraction cover, f_c (Castel, 2005).

In the full irrigation treatment (T100), irrigation dose (*Id)* replaced about 110%*IN* in 2009 and 100%*IN* in 2010 and 2011, whereas in the two RDI treatments, *Id* was scaled to a total amount of

60%*IN* (T60) and 40%*IN* (T40), only during the phase II of fruit growth (initial fruit enlargement phase, occurring from July 13 to September 13 in 2009, from July 12 to August 30 in 2010 and finally, from July 12 to August 28 in 2011), being the plots irrigated as T100 during the remaining periods of the year.

Irrigation water was automatically supplied by a drip system consisting of two drip lines per tree row laid on the soil surface at a distance of approximately 0.9 m from the row, including eight 7.4 l h^{-1} pressure-compensating emitters per single tree. One flow meter per irrigation treatment recorded the exact volumes of water applied during each irrigation event, whose frequency ranged between two irrigations per week during winter and six irrigation per week during summer. In the period when deficit irrigation was applied ~~in~~ T60 and T40, water in the soil was restored every 1-2 day.

The soil textural class, according to USDA, is sandy loam, with sand and clay contents ranging between 46-60% and 18-22% respectively. The fertilizer application was the same in all the plots, with a seasonal application of 260, 65 and 130 kg ha^{-1} of N, P_2O_5 and K_2O respectively, from April to October.

Meteorological data were acquired from a standard weather station located about 500 m apart the experimental orchard and belonging to the Irrigation Technology Service (STR) of Valencian Institute of Agrarian Research (IVIA).

2.2. Assessment of soil and crop water status

In each treatment, soil water content (*SWC*) was monitored along a soil profile with a FDR (Frequency Domain Reflectometry) down-hole probe (Enviroscan, Sentek), installed at distances of about 1.0 m and 0.5 m from the tree and the dripline respectively. Each probe allowed monitoring soil water content at four depths (0.1, 0.3, 0.5 ~~e~~ 0.7 m) every 15 min and then the measurements were averaged at daily time step.

Crop water status was monitored according to the Midday Stem Water Potential (*MSWP*, MPa), measured with a pressure chamber (Solfranc SF-Pres-35), approximately every week and on three trees for each treatment, by following the procedure described in Turner (1981). Determinations were carried out in at least two mature leaves, bagged in plastic bags and covered with a silver foil at minimum two hours prior the measurement.

To assess the model ability to identify the stress conditions consequent to the adopted RDI strategies, the Water Stress Integral (S_{MSWP}, MPa·day) was calculated according to Myers (1988):

$$S_{MSWP} = \left| \sum_{i=0}^{i=t} \left(\overline{MSWP}_{i,i+1} - c \right) n \right| \quad (5)$$

where $\overline{MSWP}_{i,i+1}$ is the mean midday steam water potential for any time interval (i,i+1), c is a threshold of *MSWP* below which crop water stress conditions occur and n is the number of days in the interval. The c value was subtracted from each $\overline{MSWP}_{i,i+1}$ to emphasize the relative difference of crop water status between treatments (Myers, 1988). Similarly, using FAO-56 model, the water stress integral, $S_{FAO\text{-}56}$, was calculated as:

$$S_{FAO\text{-}56} = \sum_{i=0}^{i=t} \left(1.0 - \overline{K}_{i,j+1} \right) n \quad (6)$$

where $\overline{Ks}_{i,i+1}$ is the mean stress coefficient for any interval (i,i+1), and the datum value equal to 1.0, corresponds to the minimum stress level reached in absence of water stress.

2.3. Soil and crop physical parameters for model setting

Average soil water content at field capacity and wilting point were assumed equal to 0.24 $cm^3\ cm^{-3}$ and 0.12 $cm^3\ cm^{-3}$, based on the soil water retention curves previously estimated, at different depths, on the same soil by Martì et al., (2013). The soil Available Water (*AW*) resulted therefore equal to 120 mm m^{-1}.

Reference daily evapotranspiration, ET_0, was computed by means of meteorological data and the FAO Penman-Monteith model. The basal crop coefficients, K_{cb}, were obtained from table 17 of the FAO-56 manual (Allen et al., 1998), by considering a citrus orchard characterized by a fraction cover of 70% and the absence of ground cover. The values of K_{cb} in the mid and final crop development stages were then adjusted to account for ~~not~~ standard climate conditions (minimum relative air humidity and wind speed different than 45% and 2.0 m s^{-1}). Table 1 summarizes the values of the variables used for model application and the related data sources.

Simulations were run from DOY 1 to 365 for the three investigated years, by assuming at DOY=1, a soil water content corresponding to the field capacity (SWC_{fc}=0.27 m^3 m^{-3}), as consequence of the copious rainfall occurred during each antecedent period.

Table 1

2.4. Statistical analysis for model validation

The model performance was evaluated based on the root mean square error (RMSE) and the mean bias error (MBE), defined as:

$$RMSE = \sqrt{\frac{\sum_{i=1}^{N}(X_{sim,i} - X_{obs,i})^2}{N}} \quad (7)$$

$$MBE = \frac{1}{N}\sum_{i=1}^{N}(X_{sim,i} - X_{obs,i}) \quad (8)$$

where N is the number of measured data, and $X_{sim,i}$ and $X_{obs,i}$ are the predicted and measured values of any considered variable (Kennedy and Neville, 1986).

Moreover, a Student t-test allowed evaluating the statistical differences between measured and simulated data (Kennedy and Neville, 1986):

$$t = \sqrt{\frac{(N-1)MBE^2}{RMSE^2 - MBE^2}} \quad (9)$$

For any fixed significance level, α, the differences are statistically significant if the calculated t is lower than a critical threshold, t_{crit},. In this respect, a significance level of α=0.05 was assumed.

Finally, the predictive power of the model was evaluated according to the Nash-Sutcliffe efficiency coefficient, E, (Nash and Sutcliffe, 1970; Willmott, 1981):

$$E = 1 - \frac{\sum_{i=1}^{N}(X_{sim,i} - X_{obs,i})^2}{\sum_{i=1}^{N}(X_{obs,i} - \overline{X_{obs}})^2}$$

A perfect match between simulated and observed data is represented by E=1, whereas for E=0 the model prediction has the same accuracy of the measured mean; values of the efficiency coefficient lower than 0 indicate that the mean of measured values is a better predictor than the considered model.

3. Results and Discussion

3.1. Agro-environmental characteristics and assessment of water saving strategies

Figure 1a-f shows the dynamic of daily standard meteorological variables, acquired during the considered years. On the other side, table 2 summarizes the main climate variables, irrigation depths, as well as the soil and crop water status evaluated during the whole considered years and in the periods of restricted irrigation water application (approximately from mid of July to the beginning of September).

As can be observed, during the considered years there was a certain variability in the rainfall distribution, that was characterized by yearly values ranging between 840 mm in 2009 and only 566 mm in 2010 (fig. 1f); on the other hand, even if the distribution of reference evapotranspiration, ET_0, was similar during the three years, with daily peaks between 5.5 mm and 6.5 mm generally occurring in July (fig. 1d), slight differences were observed in cumulated yearly values, equal to 1202 mm, 1132 mm and 1067 mm in 2009, 2010 and 2011, respectively. The total irrigation depths supplied in treatment T100 ~~resulted~~ quite variable in the three years and ranging between 512 mm

in 2009, and 315 mm in 2011. Of course, during the three years, T60 and T40 received a total irrigation depth lower than T100, as a consequence of the minor volumes applied during the periods of water restrictions. However, it has to be noticed that in 2009 the total volumes provided in the three treatments were considerably higher if compared to the other two seasons; during the first year, in fact, experiments permitted tuning the system in order to identify the duration of watering and therefore the actual volume to provide during each irrigation event.

Figure 1a,f

Table 2

During the periods of water restrictions, total rainfall, P, and reference evapotranspiration, ET_0, ~~resulted~~ equal to 19.7 mm and 405.0 mm in 2009, higher than those registered in the corresponding periods of 2010 and 2011. On average during the three years, *MSWP* in T100 ranged between -1.00 MPa and -1.17 MPa, whereas in T60 varied between -1.05 MPa and -1.65 MPa and finally, in T40, between -1.14 MPa and -1.98 MPa. According to the *MSWP* thresholds suggested by Goldhamer (2012), these values evidenced mild stress levels in treatments T100 (*MSWP*>-1.5 MPa), and slightly higher stress levels in T60 and T40 in which, however, only occasionally the stress conditions become severe (*MSWP*<-2.0 MPa).

As can be observed in table 2 the minimum values of *MSWP* observed during the periods of restricted water applications ~~tend to decline~~ at decreasing irrigation amount. Similar results can be obtained when considering the water-stress integral (S_{MSWP}, MPa·day), evaluated with eq. 5, by assuming a value of c=-1.0 MPa (Gasque et al. 2016) in agreement with González-Altozano and Castel, 1999, corresponding approximately to the maximum *MSWP* measured in the field (table 2).

For the three treatments, figure 2 shows the values of water-stress integral, S_{MSWP}, during the periods of water restriction versus the total provided irrigation depths. As can be observed, the

value of S_{MSWP} ~~decrease~~ at increasing irrigation depth, being T100 characterized by very low values of the dependent variable. The robust relationship between the two variables, characterized by a regression coefficient R^2=0.82 (significant at $p<0.01$ level according to the Pearson's correlation coefficient), confirms that S_{MSWP} can be considered a good indicator of the plant-water relationships, as suggested by Garcia-Tejero et al. (2010). Thus, in absence or under limited precipitation, this indicator can be used to predict the total irrigation depth to apply in order to achieve a desired stress level during the phase II of fruit growth (Goldhamer, 2012).

However, it has to be noticed that this relationship is influenced by the threshold value, *c*, assumed in eq. 5 and its precision is affected by the time step during which *MSWPs* are measured. In order to improve the estimation of S_{MSWP} is therefore necessary to carefully estimate the value of *c*, as well as to increase the acquisition frequency of *MSWP* even by using new sensors, like the non-invasive Zim-probe (Zimmermann et al., 2008, 2010) or field spectroscopy (Rallo et al., 2014b). Further experiments should be related to identify the consequences that the assumption of the coefficient *c* may have on the qualitative and quantitative characteristics of the productions.

Figure 2

When considering the average depth applied in each irrigation event and in the periods of water restriction, the values of S_{MSWP} are still correlated with the average irrigation depth, with a slope of the regression curve that declines at increasing ~~of~~ irrigation depth (fig. 3). Under the examined frequency of watering therefore, the values of S_{MSWP} also depends on how irrigation was managed and particularly on the average irrigation depth provided in each watering.

Figure 3

3.2. Soil-plant water relations and crop response to water deficit

Figure 4 shows the values of measured *MSWPs* as a function of the corresponding soil water status evaluated distinctly at the four different soil depths (0.1 m, 0.3 m, 0.5 m, 0.7 m) and expressed in terms of soil water content (*SWC*) or depletion (*D*). The values of *SWC* were determined as the average of 48 records acquired per day (one measurement every 30 minutes) during the period of water restriction, and can be considered representative of a soil layer with a thickness of about 10 cm (Provenzano et al., 2015).

Figure 4

As can be observed, the eco-physiological crop response to soil water deficit was quite different for the investigated soil layers and treatments. When considering the soil top-layer, the evaporative process was dominant if compared to the root water uptake, so that *MSWP* did not depend on soil water status. At ~~the~~ higher depths, where root water uptake was largely concentrated, crop water status was affected by soil water content, especially for treatment T40, characterized by the largest variability of the investigated variables. However, if considering the average soil water contents of the whole soil profile, figure 5 shows the variability between *MSWP* and the average soil water status. As can be noticed, at higher soil water contents, *MSWPs* are dispersed around to a value of -1.0 MPa and tend to decline at decreasing *SWCs*. Even though it is quite difficult to identify a clear threshold of depletion, the value of D^*≈20 mm, corresponding to a SWC^*≈0.22 can be assumed as the critical threshold for the considered soil. This threshold separates two different plant behaviors: i) $D<D^*$ for which *MSWPs* are approximately constant and equal to -1.0 MPa, expressing a condition of absence or limited water stress (González-Altozano and Castel, 1999) and ii) $D>D^*$ for which the lower is the depletion, the smaller is the *MSWP* as a consequence of the progressively increasing crop water stress.

The recognized variability of *MSWP* with soil water status is reproduced, in a certain way, by the crop water stress function schematized by FAO-56 model, according to which any reduction of plant transpiration (stress coefficient), K_s, occurring for $D>RAW$, is linearly related to the depletion D (eq. 4). For the investigated soil-crop system however, the observed depletion threshold correspond to a coefficient p of eq. 4 of about 0.2, lower than p=0.5 proposed in table 22 of FAO-56 paper (Allen et al., 1998).

Figure 5

3.3. Validation of FAO-56 model and identification of crop water stress conditions

Figure 6 shows the rainfall events during the three years (upper row), the temporal dynamic of observed (average) and simulated soil water contents, *SWC*, as well as the irrigation depths provided in 2009, 2010, and 2011 (from left to right), for treatments T100, T60 and T40 (from up to down). Standard deviations of measured *SWCs* are also indicated. As can be observed, for all the treatments, the model predicts fairly well the average soil water contents in the root zone measured during the considered periods.

Figure 6

For treatment T100, the temporal variability of average *SWC* in the root zone resulted in general more limited than the other two treatments, as a consequence of the higher irrigation volumes applied. The average *SWCs* ranged between 0.24 cm^3 cm^{-3} and 0.30 cm^3 cm^{-3}, except ~~that~~ for short periods when they ~~resulted~~ slightly lower. This circumstance evidences that the average soil water content of the soil profile was generally higher than field capacity (SWC_{fc}=0.24 m^3 m^{-3}), with values sometimes close to saturation. On the other hand, the dynamic of *SWC* in T60 and T40 during the examined years resulted quite different, in line with the rainfall events and the applied amount of

irrigation. In both these treatments, the average *SWCs* resulted slightly lower than the field capacity for long periods of the ~~examined years even if~~, however, evident reductions of water availability in the soil profile occurred, mainly in the second semester of 2010 and only episodically in 2011. It is interesting to notice that during the periods of water restriction, the dispersion of measured *SWCs* generally increased at decreasing *SWCs*, due to the partial wetting of soil profile occurring in *RDI* treatments (T60 and T40).

Table 3 shows the statistical parameters associated to the comparison between simulated and measured soil water contents, obtained for the three treatments during the whole period of observation.

Table 3

As can be observed, the values of root mean square errors always lower than 0.04 m^3 m^{-3} ~~evidenced~~ that there was a substantial agreement between the average soil water contents in the soil layer from 0.1 m to 0.7 m depth and the corresponding values simulated by the model.

According to the Student t-test, the observed differences between measured and simulated *SWCs* in the three treatments ~~resulted~~ statistically not significant at a significance level of α=0.05.

According to the statistical analysis therefore, it is evident that FAO-56 model can be considered suitable to reproduce the temporal variability of soil water content in the root zone. This result, joint to an accurate analysis of crop response to water stress, can be used for irrigation scheduling purposes, by avoiding costly and time-consuming field monitoring. Similar results have been recently obtained ~~even~~ for drought tolerant crops like olive trees (Rallo et al., 2014a) for which, however, it was necessary to implement on FAO-56 model, a more suitable crop response function to water stress.

The ability of the model to identify the actual water stress conditions occurring in RDI treatments, was assessed according to the observed similarity between measured midday stem water potentials, *MSWP*, and simulated crop water stress coefficient, K_s, evaluated as the ratio between actual and maximum transpiration simulated by the model.

Figures 7 and 8 show, respectively for T60 and T40 treatments, the temporal dynamics of reference evapotranspiration, precipitation and irrigation events, (upper row), as well as measured midday stem water potentials, *MSWP*, and simulated crop water stress coefficient, K_s, (middle row). In the lowest row of the figure, the cumulated water stress integrals during the periods of water restriction, expressed in terms of measured *MSWP* or simulated *Ks* and determined according to eqs. 5 and 6, are also shown.

As can be detected, in both treatments the absolute values of *MSWP* generally spread around 1.0 MPa for the most of examined years, identifying conditions of negligible water stress (González-Altozano and Castel, 1999), except that in the periods of water restriction, coincident with the phase II of the fruit growth (Gasque et al., 2016). During such periods and in both RDI treatments in fact, it can be noticed that *MSWPs*, after an initial decline, ~~follow~~, patterns ~~depending~~ on the water supply (irrigation or rainfall). During the three years, the minimum absolute values of *MSWP* resulted equal to -1.30, -2.09 and -1.53 MPa in T60, and equal to -1.48, -2.50 and -1.95 MPa in T40. The lowest crop water stress observed in 2009 ~~is~~, an obvious consequence of the higher irrigation volumes provided, as previously discussed.

When considering the model results in terms of simulated stress coefficient K_s, it can be easily verified that this indicator ~~allows~~ explaining the variability of measured *MSWPs*. As can be observed in fact, the dynamic of K_s coefficient follows the temporal patterns of *MSWP*, as a consequence of the correct schematization of the stress function under crop water deficit conditions. Even considering the cumulative values of the water stress integral, S_{cum}, during the water restriction periods (lowest row of figs. 7 and 8), it is possible to notice that the modeled $S_{cum,FAO-56}$

values fit fairly well to the measured $S_{cum,MSWP,}$ confirming the ability of the model to identify the differences, in terms of temporal patterns of water stress integral, recognized among the treatments.

Figure 7

Figure 8

Figure 9a shows the measured Midday Stem Water Potential (absolute values), *MSWP*, as a function of the simulated water stress coefficient, K_s, during the periods of water restriction, whereas figure 9b illustrates the comparison between cumulated water stress integrals evaluated according to measured *MSWP* ($S_{cum,MSWP}$) and simulated K_s ($S_{cum,FAO-56}$), based on a weekly time step.

As can be noticed in figure 9a the two variables are linearly correlated, with intercept and angular coefficient equal to 2.14 MPa and -1.14 MPa (R^2=0.73), respectively. This relation allows extrapolating the -2.0 MPa of MSWP proposed as threshold value in this same orchard (Gasque et al., 2016) to a K_s of 0.12. On the other hand, when considering the cumulative values of the water stress integral (fig. 9b) it can be observed that, for each treatment, a strong linear correlation exist between $S_{cum,MSWP}$ and $S_{cum,FAO-56}$. Of course, the variability ranges of both the considered variables increase at decreasing of the applied irrigation depth, as a consequence of the higher cumulated stress levels achieved by crop. In addition, even the slope of the regression relationships, depending on the adopted irrigation strategy, increases at increasing of the cumulative stress levels, underlining the sensitivity of the model to identify the observed variability of crop water status, characterizing the different examined treatments.

This last result indicates that under the examined conditions the model can be successfully used to indirectly estimate and with a fairly good approximation, the cumulative stress occurring in the field during the phase II of fruit growth and corresponding to any pre-fixed irrigation strategy.

Figure 9 a,b

Conclusions

In the paper, the eco-physiological response of citrus orchard to soil water deficit conditions was investigated ~~according to~~ three years ~~of~~ field measurements of soil and plant water status, carried out in a commercial citrus orchard located near the town of Senyera, Spain. Three different irrigation treatments, including one full irrigation (T100) and two regulated deficit irrigation were in particular examined. In the ~~latters~~, irrigation water supply was scheduled according to different percentage of irrigation needs (T60 and T40) applied only during the phase II of fruit growth (approximately from mid of July to the ~~begin~~ of September), ~~being~~ the crop irrigated ~~as~~ T100 during the other periods of the year. Soil water status was expressed in terms of soil water content (*SWC*) or depletion (*D*), whereas crop water status considered the midday ~~steam~~ water potentials (*MSWP*) measured in the field, as well as the water stress integral evaluated in the periods of water restriction.

Experimental data evidenced the absence of stress in treatment T100 and mild or moderate stress levels in T60 and in T40 in which, however, conditions of severe stress were only occasionally achieved. The analysis ~~allowed identifying the~~ strong correlation ~~existing~~ between the water stress integral and the applied irrigation depth, which can be used to predict the seasonal irrigation volumes to be provided when a desired crop stress level is required.

On the other hand, *MSWPs* were dispersed around a value of -1.0MPa when the average *SWCs* in the soil profile ranged between the soil field capacity SWC_{fc}=0.24 m^3 m^{-3} and a threshold value of soil water content of SWC^*≈0.22m^3 m^{-3}, corresponding to a soil depletion D^*≈20 mm. At values of SWC≤0. 22 m^3 m^{-3}, *MSWP* ~~resulted~~ linearly decreasing at decreasing *SWC* (increasing *D*), as a consequence of the gradually rising crop water stress.

Finally, the performance of FAO-56 model to identify the temporal dynamic of soil and crop water

status, under different irrigation strategies, was demonstrated. The comparison between measured and simulated soil water contents in the root zone evidenced that the model is able to predict, with reasonable accuracy, the average *SWC* in the root zone, with differences statistically not significant and errors of estimation always lower than 0.04 m^3 m^{-3}. On the other hand, the model ability to predict the actual crop water stress was demonstrated according to the observed similarity between the temporal dynamic of the simulated water stress coefficient (K_s) with the measured midday stem water potentials, *MSWP*. In fact, it was observed that the temporal variability of *MSWP* can be explained by the dynamic of simulated K_s.

Even extending the analysis to crop water stress cumulated during periods of water restriction, it was observed how the model predictions fitted quite well to the corresponding measured, confirming the suitability of the model to identify the differences, in terms of temporal pattern of water stress integral, characterizing the examined treatments.

After a site-specific calibration accounting for different irrigation strategies therefore, the cumulative water stress integral evaluated by the model can be used as a surrogate variable of *MSWP* for irrigation timing established according to "model-based" irrigation scheduling, even under periods of water restrictions.

Acknowledgements

Research was carried out in the frame of the PRIN 2010 projects, co-financed by Ministero dell'Istruzione, dell'Università e della Ricerca (MIUR) and Università degli Studi di Palermo. Authors wish to thank the Committee for International Relations Office (CORI) of University of Palermo to support the research cooperation with the Polytechnic University of Valencia.

Contributions to the manuscript have to be shared between the authors as follows: Experimental setup and field data acquisition were handled by Pablo González-Altozano and Juan Manzano-

Juárez, whereas data processing and text writing were cared by Giovanni Rallo and Giuseppe Provenzano. All the Authors contributed to the final revision of the paper.

References

Allen, R. G., L.S. Pereira, D. Raes, M. Smith. 1998. Crop evapotranspiration - Guidelines for computing crop water requirements. FAO Irrigation and Drainage Paper 56 , Food and Agriculture Organization, Rome, Italy.

Barragan, J., Bralts V., Wu I.P. 2006. Assessment of Emission Uniformity for Micro-irrigation Design. Bio. Eng., 93(1), 89-97. http://dx.doi.org/10.1016/j.biosystemseng.2005.09.010.

Cammalleri C., G. Ciraolo, M. Minacapilli, G. Rallo. 2013. Evapotranspiration from an Olive Orchard using Remote Sensing-Based Dual Crop Coefficient Approach. Water Resources Management. 27(14), 4877-4895.

Castel, J.R., 2005. Evapotranspiración, balance de energía y coeficiente de cultivo de plantaciones de cítricos en Valencia. Monografías INIA 17, 210-219.

Cohen, A., A. Goell. 1988. Fruit growth and dry matter accumulation in grape fruit during periods of water with holding and after re-irrigation. Australian J. Plant Physiology. 15, 633-639.

Consoli, S., G.L. Cirelli, A. Toscano. 2006. Monitoring crop coefficient of orange orchards using energy balance and the remote sensed NDVI. Proceedings of the Conference on "Remote Sensing for Agriculture, Ecosystems, and Hydrology", Stockolm, Sweden.

Costa, J.M., M.F. Ortuño, M.M. Chaves. 2007. Deficit irrigation as strategy to save water: Physiology and potential application to horticulture. J. of Integrative Plant Biology. 49, 1421–1434.

de la Hera, M.L., P. Romero, E. Gómez-Plaza, E. Martinez-Cutillas. 2007. Is partial root-zone drying an effective irrigation technique to improve water use efficiency and fruit quality in field grown wine grapes under semiarid conditions? Agricultural Water Management. 87, 261-274.

de Souza, C. R., J.P. Maroco, T. P. dos Santos, M. L. Rodrigues, C. Lopes, J.S. Pereira, M.M. Chaves. 2005. Control of stomatal aperture and carbon uptake by deficit irrigation in two grapevine cultivars. Agriculture, Ecosystems & Environment. 106(2–3), 261-274, ISSN 0167-

8809, http://dx.doi.org/10.1016/j.agee.2004.10.014.

Eurostat, 2014. Agricultural production - Orchards. In Agriculture, forestry and fishery statistics. http://ec.europa.eu/eurostat/statistics-explained/index.php/Agricultural_production_-_orchards

García-Tejero I., J.A. Jiménez-Bocanegra, G. Martínez, R. Romero, V.H. Durán-Zuazo, J.L. Muriel-Fernández. 2010. Positive impact of regulated deficit irrigation on yield and fruit quality in a commercial citrus orchard [Citrus sinensis (L.) Osbeck, cv. salustiano]. Agricultural Water Management. 97(5), 614-622.

Gasque, M., P. Martí, B. Granero, P. González-Altozano. 2016. Effects of long-term summer deficit irrigation on 'Navelina' citrus trees. Agricultural Water Management. 169, 140-147.

Goldhamer, D. 2012. Citrus in Crop Yield Response to Water. FAO Irrigation and Drainage Paper No. 66. In P. Steduto, T.C. Hsiao, E. Fereres, and D. Raes, eds. Food and Agriculture Organization of the United Nations, Rome, Italy, 246:296.

González-Altozano, P., J.R. Castel. 1999. Regulated deficit irrigation in 'Clementina de Nules' citrus trees. I: Yield and fruit quality effects. J. Horticultural Science and Biotechnology. 74 (6), 706-713.

Hutton, R.J., J.J. Landsberg, G. Sutton. 2007. Timing irrigation to suit citrus phenology: a means of reducing water use without compromising fruit yield and quality? Australian J. Experimental Agriculture. 47,71-80.

Kennedy, J.B., A.M. Neville. 1986. Basic Statistical Methods for Engineers and Scientists, Third Edition, New York, Harper & Row.

Marsal, J., M. Mata, J. Del Campo, A. Arbonés, X. Vallverdú, J. Girona, N. Olivo. 2008. Evaluation of partial root-zone drying for potential field use as a deficit irrigation technique in commercial vineyards according to two different pipeline layouts. Irrigation Science. 26, 347-356.

Martí, P., M. Gasque, P. González-Altozano. 2013. An artificial neural network approach to the

estimation of stem water potential from frequency domain reflectometry soil moisture measurements and meteorological data. Computers and Electronics in Agriculture. 91, 75-86.

Merriam, J.L. 1966. A management control concept for determining the economical depth and frequency of irrigation. Trans. of the ASAE. 9, 492-498.

Minacapilli, M., C. Agnese, F. Blanda, C. Cammalleri, G. Ciraolo, G. D'Urso, M. Iovino, D. Pumo, G. Provenzano, G. Rallo. 2009. Estimation of actual evapotranspiration of Mediterranean perennial crops by means of remote-sensing based surface energy balance models. Hydrology and Earth System Science. 13, 1061-1074, doi:10.5194/hess-13-1061-2009.

Myers, B.J. 1988. Water stress integral. A link between short-term stress and long-term growth. Tree Physiology. 4, 315-323.

Nash, J.E., J.V. Sutcliffe. 1970. River flow forecasting through conceptual models part I: A discussion of principles. Journal of Hydrology. 10(3), 282-290.

Provenzano, G., G. Rallo, H. Ghazouani. 2015. Assessing Field and Laboratory Calibration Protocols for the Diviner 2000 Probe in a Range of Soils with Different Textures. J. Irrigation and Drainage Engineering. 10.1061/(ASCE)IR.1943-4774.0000950, 04015040.

Provenzano G., Rodriguez-Sinobas L., Tarquis A.M.. 2013. Soil and Irrigation Sustainability Practices. Agricultural Water Management. 120, 1-4. DOI.org/10.1016/S0378-3774(13)00039-5.

Rallo, G., C. Agnese, M. Minacapilli, G. Provenzano. 2012. Comparison of SWAP and FAO Agro-Hydrological Models to Schedule Irrigation of Wine Grapes. J. Irrigation and Drainage Engineering. 138(7), 581-591.

Rallo, G., G. Baiamonte, J. Manzano, G. Provenzano. 2014a. Improvement of FAO-56 Model to Estimate Transpiration Fluxes of Drought Tolerant Crops under Soil Water Deficit: Application for Olive Groves. J. Irrigation and Drainage Engineering. 140. Special Issue: Trends and Challenges of Sustainable Irrigated Agriculture, A4014001.

Rallo, G., Minacapilli, M., Ciraolo, G., Provenzano, G. 2014b. Detecting crop water status in mature olive groves using vegetation spectral measurements. Biosystems Engineering, 128, pp. 52-68.

Rallo, G., G. Provenzano. 2013. Modelling eco-physiological response of table olive trees (Oleaeuropaea L.) to soil water deficit conditions. Agricultural Water Management. 120, 79-88. ISSN 0378-3774, http://dx.doi.org/10.1016/j.agwat.2012.10.005.

Rodrigues, M.C., T.P. Santos, A.P. Rodrigues, C.R. De Souza, C.M. Lopes, J.P. Maroco, J.S. Pereira, M.M. Chaves. 2008. Hydraulic and chemical signalling in the regulation of stomatal conductance and plant water use in field grapevines growing under deficit irrigation. Functional Plant Biology. 35, 565-579.

Romero P., I.C. Dodd, A. Martinez-Cutillas. 2012. Contrasting physiological effects of partial root-zone drying in field-grown grapevine (Vitis vinifera L. cv. Monastrell) according to total soil water availability. J. of Experimental Botany. 63, 4071-4083.

Sammis, T., P. Sharma, M.K. Shukla, J. Wang, D. Miller. 2012. A water-balance drip-irrigation scheduling model. Agricultural Water Management. 113, 30-37.

SAS Institute, 1994. SAS/STAT User's Guide. SAS Inst. Inc., Cary, NC, USA.

Smith, P., D. Martino, Z. Cai, D. Gwary, H. Janzen, P. Kumar, B. McCarl, S. Ogle, F. O'Mara, C. Rice, B. Scholes, O. Sirotenko. 2007. Agriculture. In Climate Change 2007:Mitigation. Contribution of Working Group III to the Fourth Assessment Report of the Intergovernmental Panel on Climate Change [B. Metz, O.R. Davidson, P.R. Bosch, R. Dave, L.A. Meyer (eds)], Cambridge University Press, Cambridge, United Kingdom and New York, NY, USA.

Turner, N.C. 1981. Techniques and experimental approaches for the measurement of plant water status. Plant and Soil. 58, 339-366.

Van Diepen, C. A., C. Rappoldt, J. Wolf, H. van Keulen. 1988. CWFS crop growth simulation model WOFOST. Documentation, Version 4.1, Centre for World Food Studies, Wageningen,

The Netherlands.

Willmot, C. J. 1981.On the validation of models. Physical Geography, 2,184-194.

Wu, I. P., Barragan J., Bralts V. 2006. Field performance and evaluation. In F. R. Lamm, J. E Ayars, and F. S. Nakayama (Eds.). Micro-irrigation for crop production. Elsevier, Amsterdam.

Yonemoto, Y., K. Matsumoto, T. Furukawa, M. Asakawa, H. Okuda, T. Takahara. 2004. Effects of rootstock and crop load on sap flow rate in branches of 'Shirakawa Satsuma' mandarin (Citrus unshiu Marc.). Scientia Horticulturae. 102(3), 295-300.

Zimmermann, D, R. Reuss, M. Westhoff, P. Gessner, W. Bauer, E. Bamberg, F.W. Bentrup, U. Zimmermann. 2008. A novel, non-invasive, online-monitoring, versatile and easy plantbased probe for measuring leaf water status. J. Exp. Bot. 59:3157–3167.

Zimmermann, U., S. Rüger, O. Shapira, M. Westhoff, L.H. Wegner, R. Reuss, P. Gessner, G. Zimmermann, Y. Israeli, A. Zhou, A. Schwartz, E. Bamberg, D. Zimmermann. 2010. Effects of environmental parameters and irrigation on the turgor pressure of banana plants measured using the non-invasive, online monitoring leaf patch clamp pressure probe. Plant Biol. 12:424–436.

Tables

Click here to download Tables: Table.docx

Tab. 1 – Values assumed for the variables used for FAO-56 model simulations

Model Variables	T100			T60			T40			Data source
	2009	2010	2011	2009	2010	2011	2009	2010	2011	
Average Soil water content at field capacity, SWC_{fc} [$m^3 m^{-3}$]					0.24					Martí et al., 2013
Average Soil water content at field capacity, SWC_{wp} [$m^3 m^{-3}$]					0.12					Martí et al., 2014
Available Water, AW [mm m^{-1}]					120					estimated
Depletion factor, p [%]					50					tab. 22, FAO-56 paper
Total Evaporable Water, TEW [mm]					6					tab. 19, FAO-56 paper
Readily Evaporable Water, REW [mm]					11					tab. 19, FAO-56 paper
Fraction of soil surface wetted by irrigation, f_w [-]					0.4					measured
Day of the year at time of planting, J_{plant} [-]					1					tab. 11, FAO-56 paper
Day of the year at beginning of development period, J_{dev} [-]					62					tab. 11, FAO-56 paper
Day of the year at beginning of midseason period, J_{mid} [-]					152					tab. 11, FAO-56 paper
Day of the year at beginning of late season period, J_{late} [-]					272					tab. 11, FAO-56 paper
Day of the year at time of harvest or death, J_{harv} [-]					365					tab. 11, FAO-56 paper
Canopy fraction cover. f_c [-]	0.40	0.40	0.38	0.40	0.40	0.40	0.42	0.42	0.40	estimated
Basal crop coefficient at initial season, $K_{cb\ ini}$ [-]	0.65	0.65	0.65	0.65	0.65	0.65	0.65	0.65	0.65	tab. 17, FAO-56 paper
Basal crop coefficient at mid-season, $K_{cb\ mid}$ [-], adjusted	0.56	0.56	0.55	0.56	0.56	0.55	0.56	0.56	0.55	tab. 17, FAO-56 paper
Basal crop coefficient at late-season, $K_{cb\ end}$ [-], adjusted	0.61	0.61	0.60	0.61	0.61	0.60	0.61	0.61	0.60	tab. 17, FAO-56 paper
Maximum crop height, H [m]	2.5	2.5	2.5	2.0	2.0	2.0	2.0	2.0	2.0	estimated
Minimum rooting depth, Z_r [m]	0.9	0.9	0.9	0.9	0.9	0.9	0.9	0.9	0.9	estimated
Maximum rooting depth, Z_r [m]	0.9	0.9	0.9	0.9	0.9	0.9	0.9	0.9	0.9	estimated
Midseason, Average Wind Speed [m s^{-1}]	1.3	1.2	1.1	1.3	1.2	1.1	1.3	1.2	1.1	measured
Midseason, Average RH_{min} [%]	48.0	49.0	50.0	48.0	49.0	50.0	48.0	49.0	50.0	measured

T*ab. 2- Summary of climate and irrigation variables, soil and crop water status during the three years and during the periods of water restriction. The symbols Σ, μ and σ represent the sum, the average and the standard deviation of each considered variable*

			ENTIRE YEAR									PERIOD OF WATER RESTRICTION								
			2009			2010			2011			2009			2010			2011		
			T100	T60	T40	T100	T60	T40	T100	T60	T40	T100	T60	T40	T100	T60	T40	T100	T60	T40
Climate variables	Air temperature [°C]	μ		18.0			17.0			17.8			26.9			26.8			26.4	
		σ		6.5			7.0			6.5			1.5			1.8			1.5	
	Air relative humidity [°C]	μ		67.9			69.1			71.7			65.3			67.4			67.0	
		σ		11.8			12.8			11.1			7.4			8.3			7.5	
	Wind speed at 2.0 m [m s^{-1}]	μ		1.3			1.2			1.0			1.4			1.2			1.2	
		σ		0.8			0.7			0.5			0.3			0.2			0.2	
	Global solar radiation [MJ m^{-2}]	μ		1.4			1.4			1.3			2.1			2.0			2.0	
		σ		0.7			0.7			0.7			0.4			0.5			0.4	
	Reference evapotranspiration [mm]	Σ		1202			1132			1067			405			403			388	
	Precipitation [mm]	Σ		840			566			616			19.7			11.8			2.0	
Irrigation variables	Irrigation amount [mm]	Σ	512.0	448.8	371.0	362.4	285.4	264.5	315.6	252.3	248.0	185.5	142.0	92.0	154.9	79.2	46.2	129.7	60.3	38.9
	Number of irrigation events [-]	-	164	167	159	148	148	126	145	142	142	48	48	47	44	44	31	34	34	34
	Irrigation depth [mm]	μ	3.1	2.7	2.3	2.4	1.9	2.1	2.2	1.8	1.7	3.9	3.0	2.0	3.5	1.8	1.5	3.8	1.8	1.1
		σ	1.8	1.4	1.3	1.4	1.1	1.4	1.6	1.0	1.1	1.4	1.3	1.0	1.1	0.9	0.3	1.7	0.9	0.7
Soil Water Status	Soil water content (0.1-0.7 m) [cm^3 cm^{-3}]	μ	0.26	0.24	0.24	0.26	0.23	0.24	0.27	0.24	0.24	0.25	0.24	0.21	0.27	0.22	0.20	0.29	0.25	0.21
		σ	0.02	0.01	0.02	0.01	0.02	0.04	0.01	0.03	0.03	0.01	0.01	0.00	0.01	0.01	0.02	0.01	0.01	0.02
	Depletion (0.1-0.7 m) [mm m^{-1}]	μ	17.3	26.0	33.6	19.9	39.3	31.4	5.3	27.4	31.0	26.6	27.9	55.6	12.0	51.9	66.8	0.0	21.0	62.1
Plant Water Status	Midday Stem Water Potential [MPa]	max	-0.56	-0.55	-0.56	-0.93	-0.92	-0.92	-0.83	-0.77	-0.84	-0.94	-0.93	-0.96	-1.08	-1.09	-1.22	-0.98	-1.09	-1.23
		min	-1.15	-1.30	-1.48	-1.30	-2.09	-2.50	-1.30	-1.56	-1.95	-1.13	-1.30	-1.48	-1.27	-2.09	-2.50	-1.11	-1.56	-1.95
		μ	-0.97	-0.98	-1.01	-1.08	-1.12	-1.24	-1.03	-1.11	-1.18	-1.01	-1.05	-1.14	-1.13	-1.34	-1.53	-1.04	-1.31	-1.58
		σ	-0.05	-0.04	-0.05	-0.04	-0.04	-0.05	-0.05	-0.06	-0.08	-0.05	-0.04	-0.06	-0.04	-0.04	-0.04	-0.04	-0.10	-0.13
	Water Stress Integral [MPa]	eq. 5										1.7	3.4	7.7	6.7	15.3	24.5	1.5	13.4	24.8

Tab. 3 – Results of statistical comparison between simulated and observed soil water contents during the whole period of observation

Treatment	**Number of data (N) [-]**	**Root Mean Square Error (RMSE) [m^3 m^{-3}]**	**Mean Bias Error (MBE) [m^3 m^{-3}]**	***Student-t***	t_{crit} ***(a=0.05)***
T100	837	0.040	0.002	1.17	1.96
T60	856	0.036	0.001	1.04	1.96
T40	856	0.037	0.001	1.07	1.96

Figure caption list

Fig. 1a-f - Daily values of (a) global solar radiation, R_g, (b) minimum and maximum relative air humidity, RH, (c) minimum and maximum air temperature, T_{air}, (d) wind speed at 2.0 above soil surface, v, (e) reference evapotranspiration, ET_0, and (f) precipitation, P, and cumulated P measured in 2009, 2010 and 2011

Fig. 2 – Values of water stress integral, $S_{MSWP,}$ versus the irrigation depth applied during the periods of water restriction, I, evaluated by using eq. 5 with c=-1.0

Fig. 3 - Relationship between water stress integral, S_{MSWP}, and average irrigation depth, Id, as applied during each watering

Fig. 4– Experimental values of Midday Stem Water Potential (MSWP) and corresponding soil water status expressed in terms of soil water content, SWC, and depletion, D, during the periods of water restriction. Dotted and solid vertical lines correspond to wilting point and field capacity, respectively

Fig. 5 - Midday Stem Water Potential (MSWP) as a function of the average soil water status in the layer 0.1-0.7 m, expressed in terms of average soil water content, SWC, or Depletion, D. Dotted and solid vertical lines correspond to wilting point and field capacity, respectively. The crop water stress function, $K_s(D)$, proposed by FAO-56 is also represented in the secondary axes (dashed line)

Fig. 6 - Temporal dynamic of precipitation (upper row), irrigation events, observed and simulated soil water content for the three treatments, T100, T60 and T40 (from up to down), during the three years (from left to right). The standard deviations of measured values, $\pm\sigma$, are also indicated with grey bars.

Fig. 7 - Temporal dynamic of: i) reference evapotranspiration, ET_0, precipitation, P, and irrigation, I, events (upper row); ii) measured midday stem water potentials, MSWP, and simulated water stress coefficient, K_s (central row); iii) measured and simulated water stress integral, S_{cum}, during the periods of water restriction (lower row), referred to T60 treatment

Fig. 8 - Temporal dynamic of: i) reference evapotranspiration, ET_0, precipitation, P, and irrigation, I, events (upper row); ii) measured midday stem water potentials, MSWP, and simulated water stress coefficient, K_s (central row); iii) measured and simulated water stress integral, S_{cum}, during the periods of water restriction (lower row), referred to T40 treatment

Fig. 9 a,b - a) Relationship between measured Midday Stem Water Potential, MSWP, and simulated water stress coefficient, K_s, obtained during the periods of water restriction. b) Measured cumulated water stress (S_{MSWP}) during two consecutive measurements (weekly time step) as a function of the corresponding simulated water stress (S_{FAO-56})

Figure1

Click here to download high resolution image

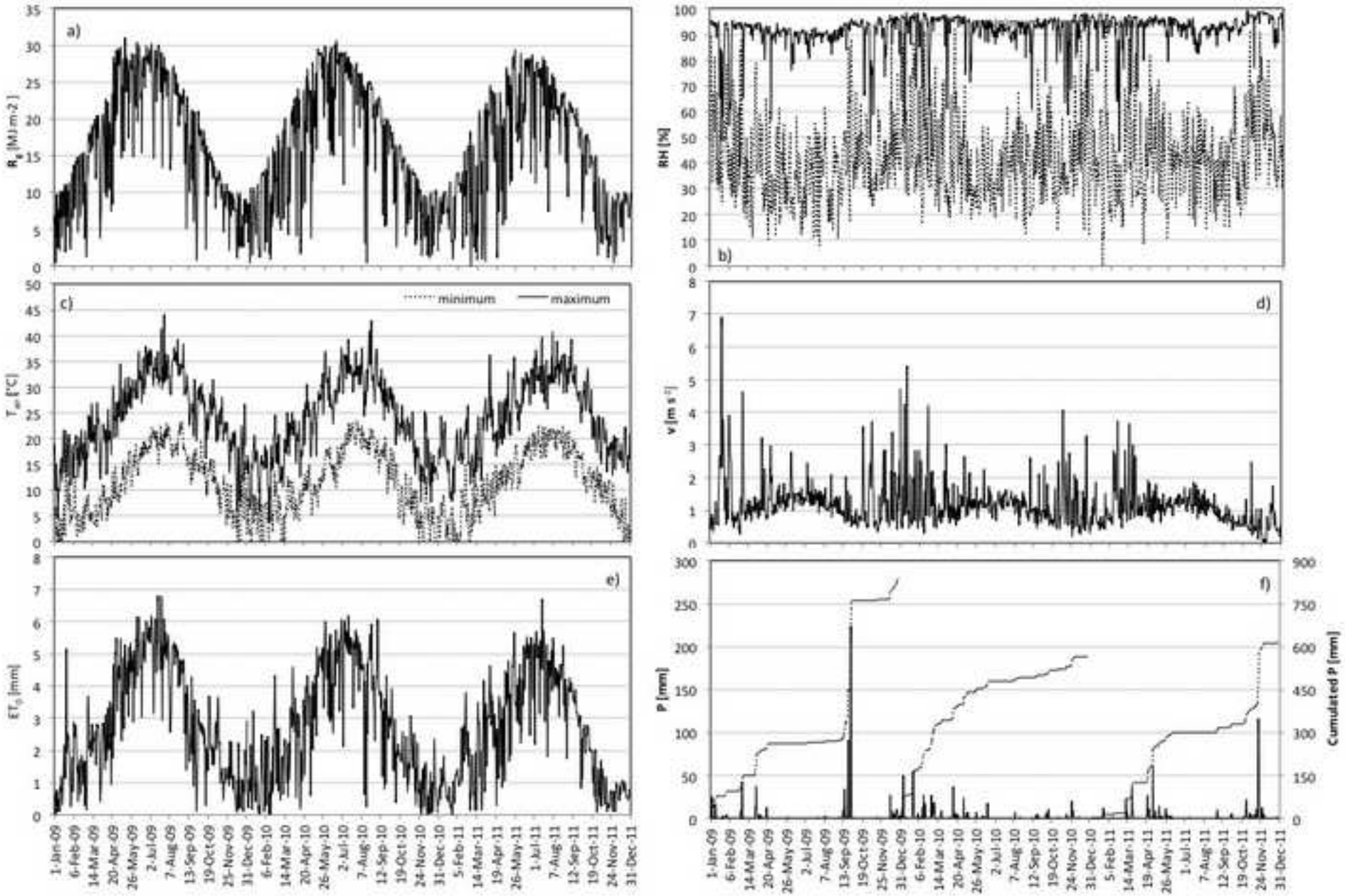

Figure2

Click here to download high resolution image

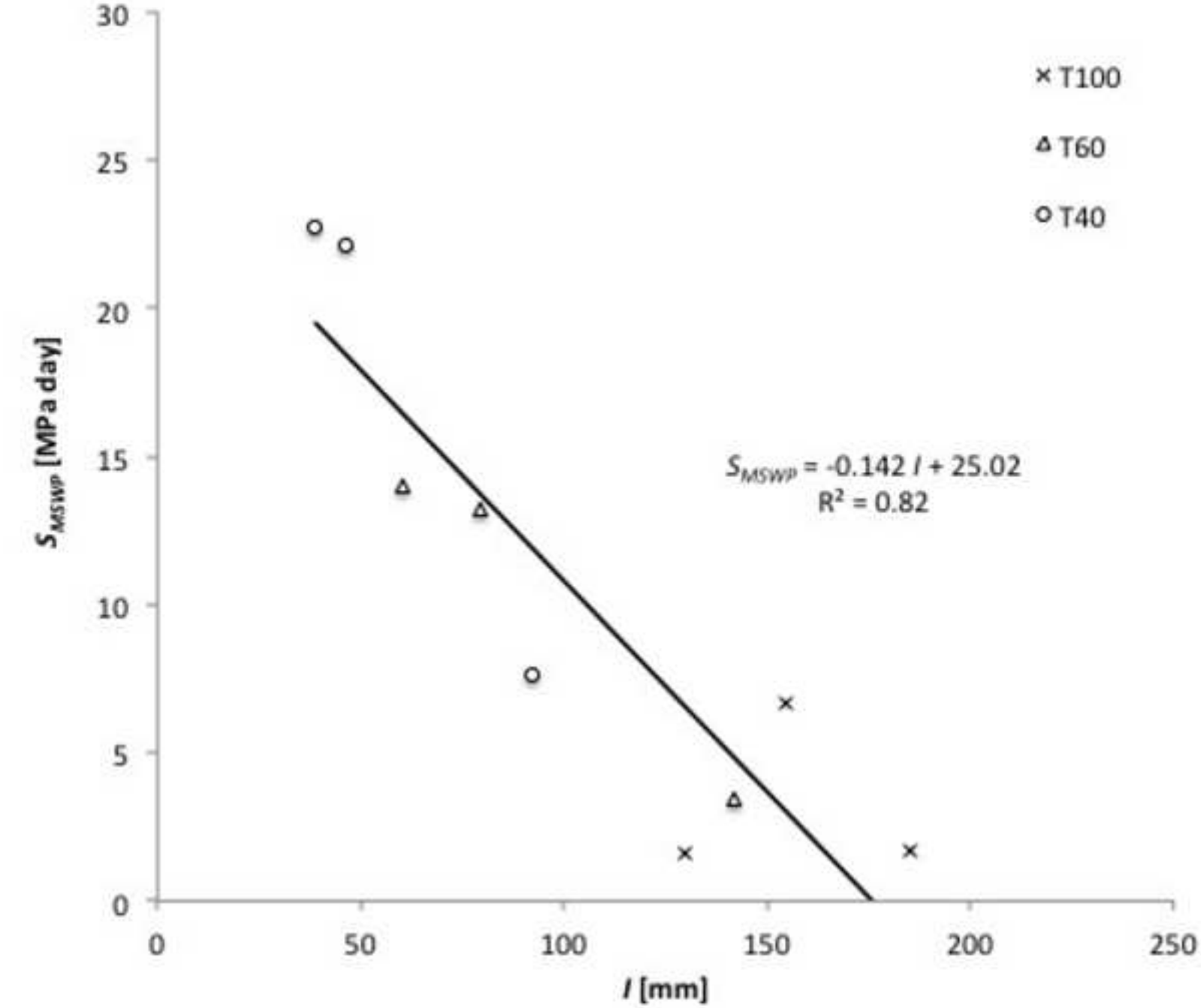

Figure3

Click here to download high resolution image

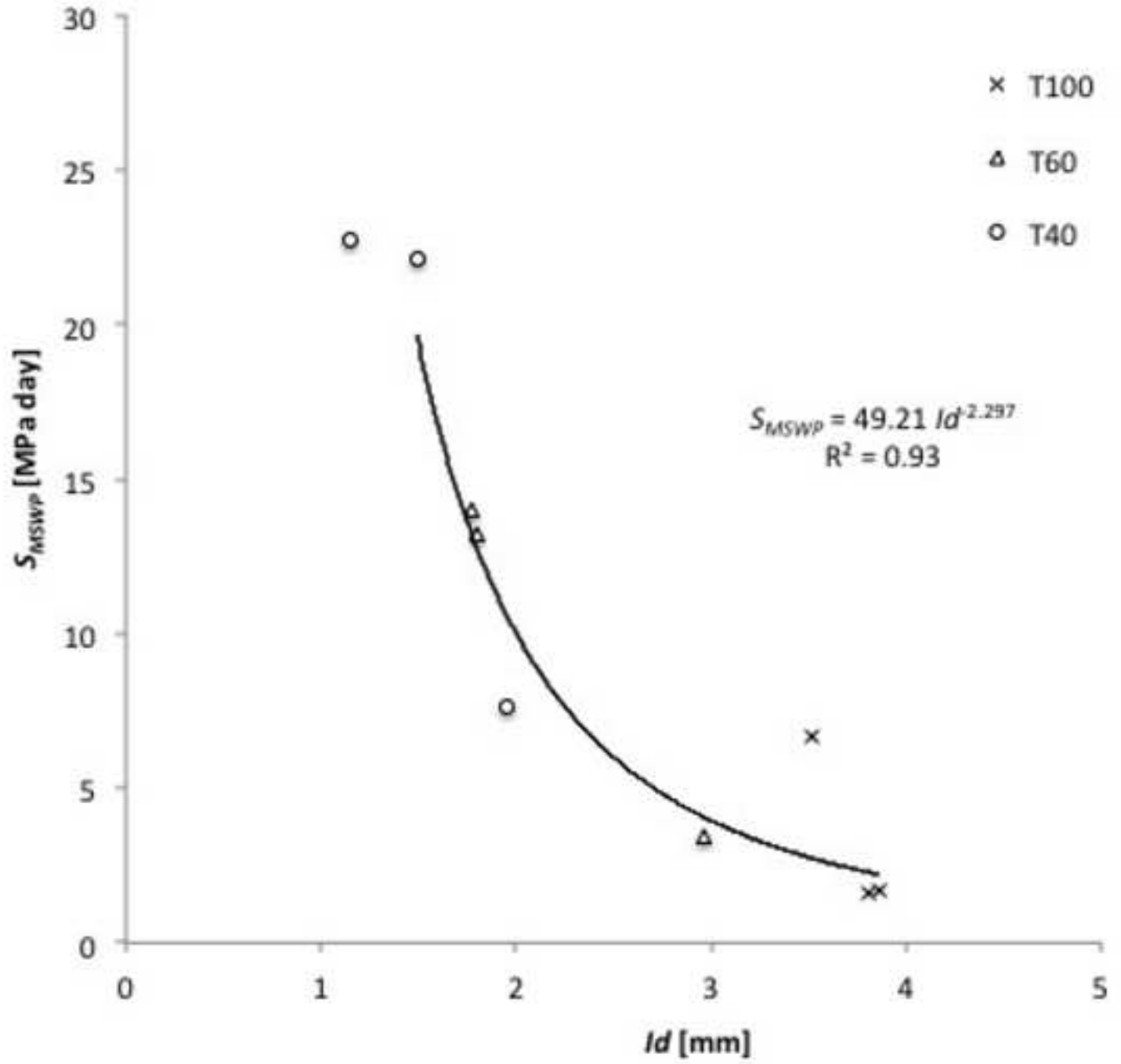

Figure4

Click here to download high resolution image

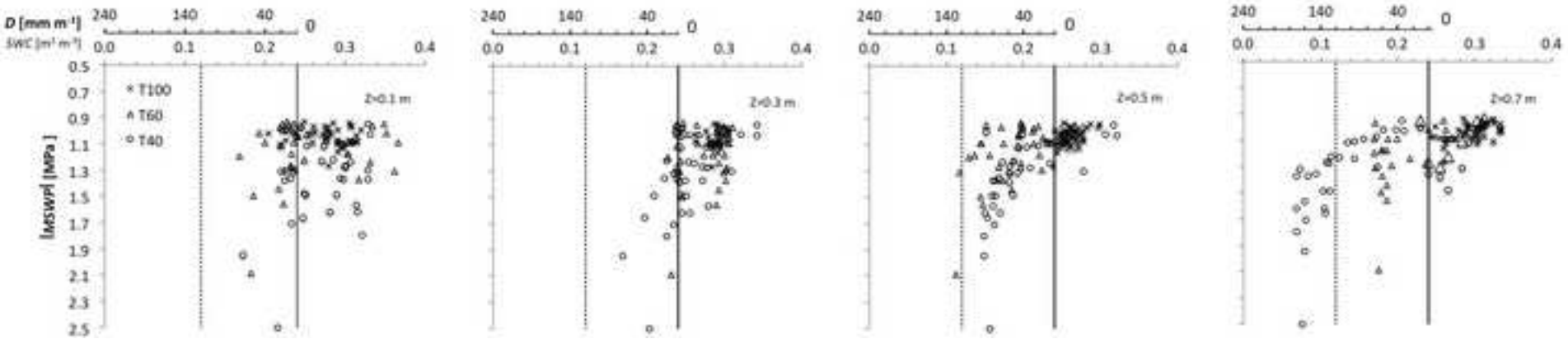

Figure5

Click here to download high resolution image

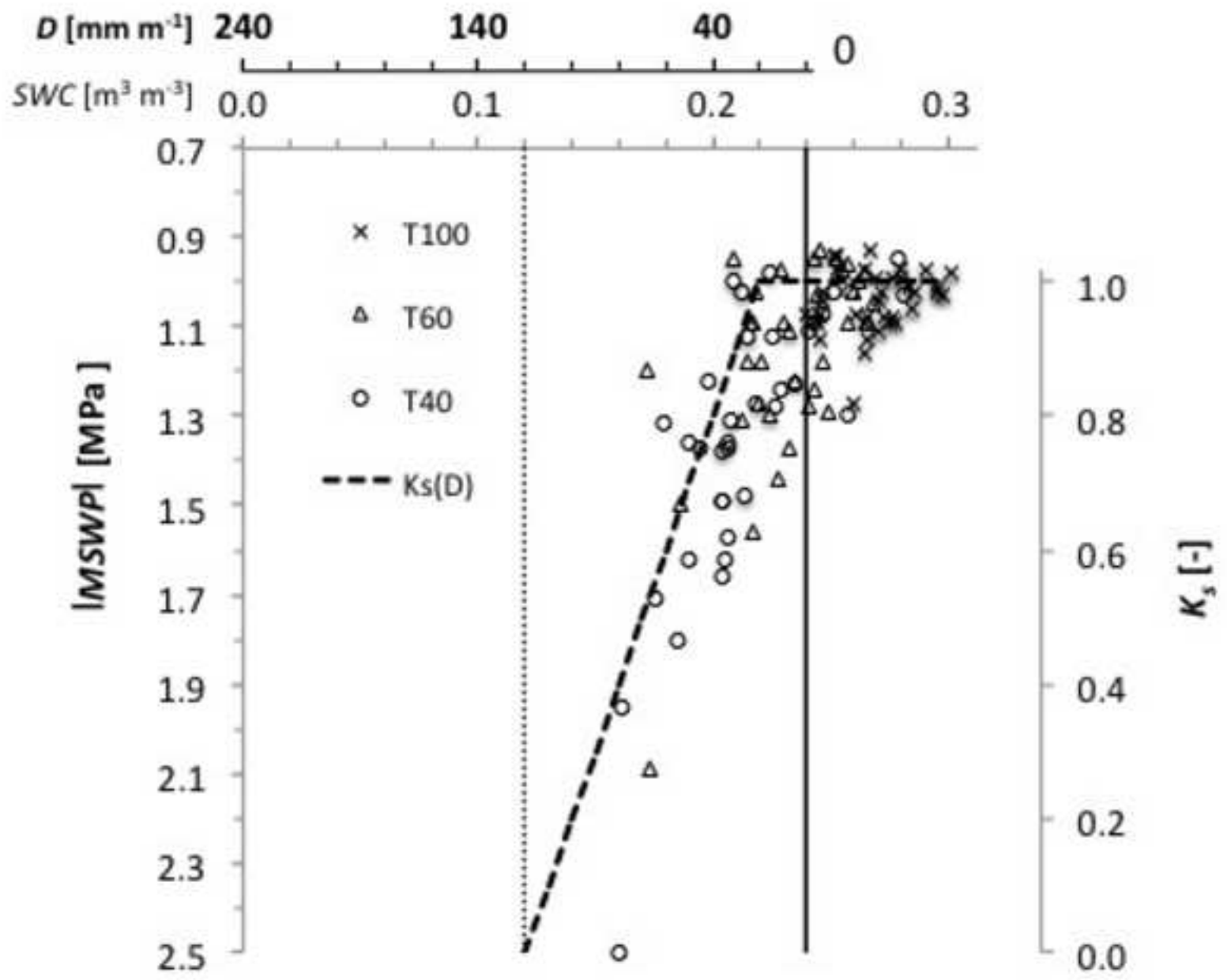

Figure6

Click here to download high resolution image

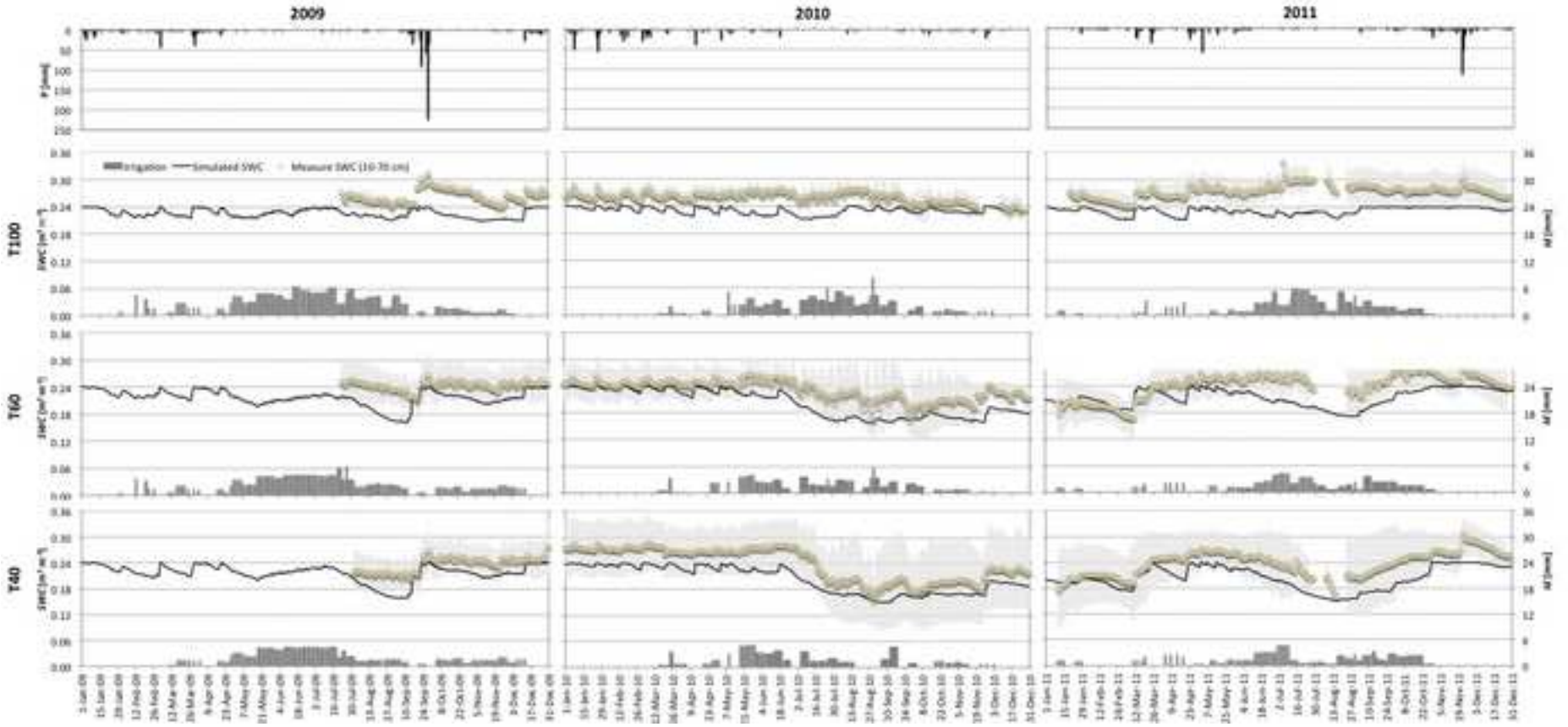

Figure7

Click here to download high resolution image

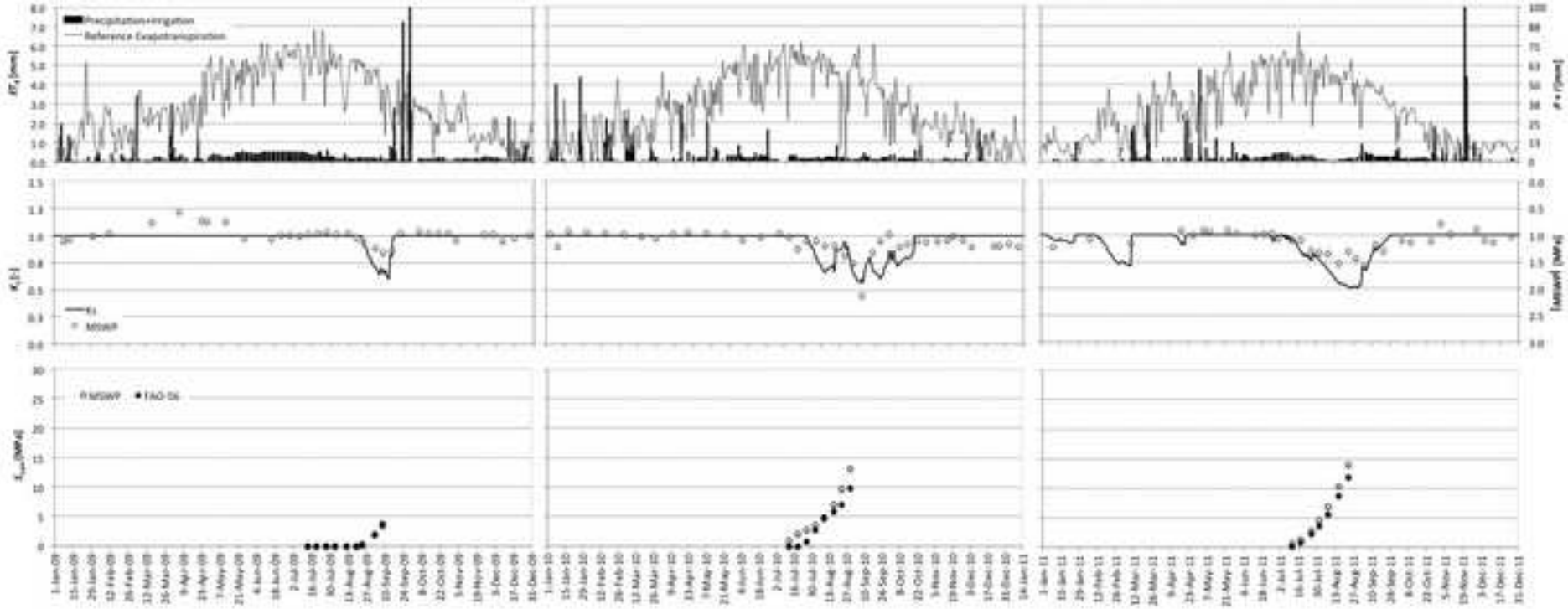

Figure8

Click here to download high resolution image

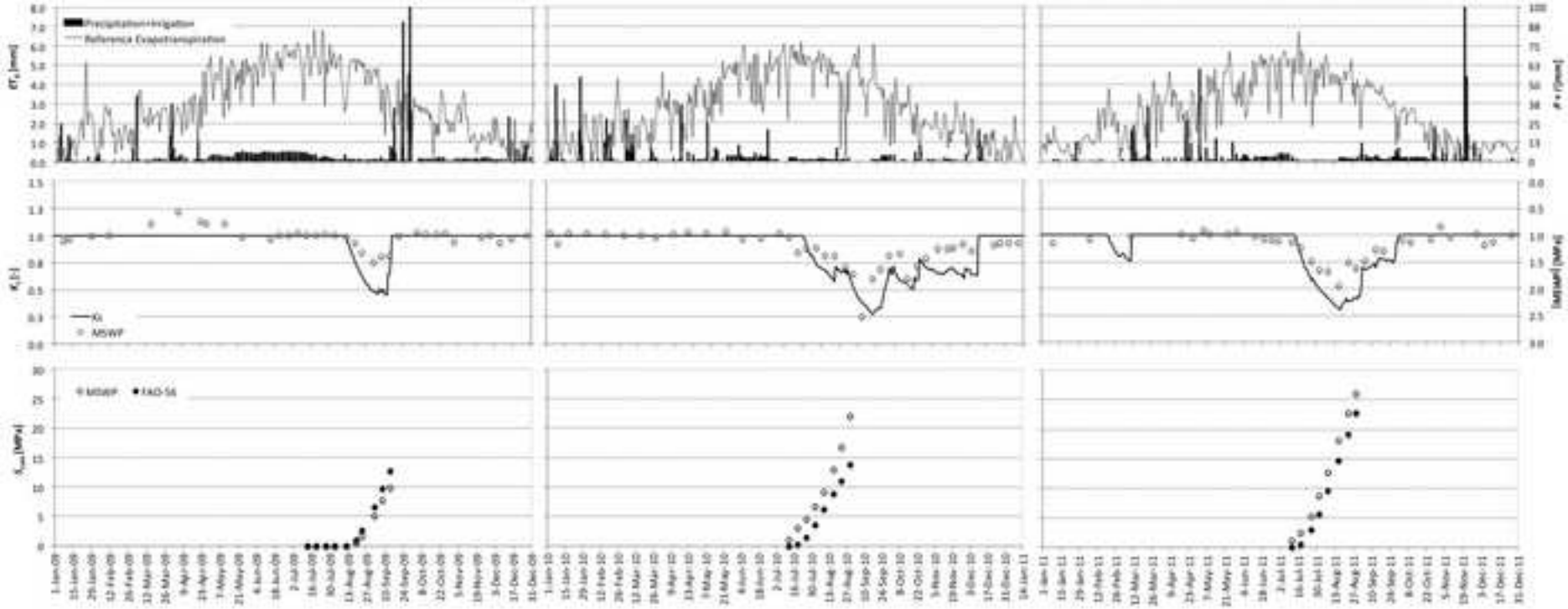

Figure9

Click here to download high resolution image